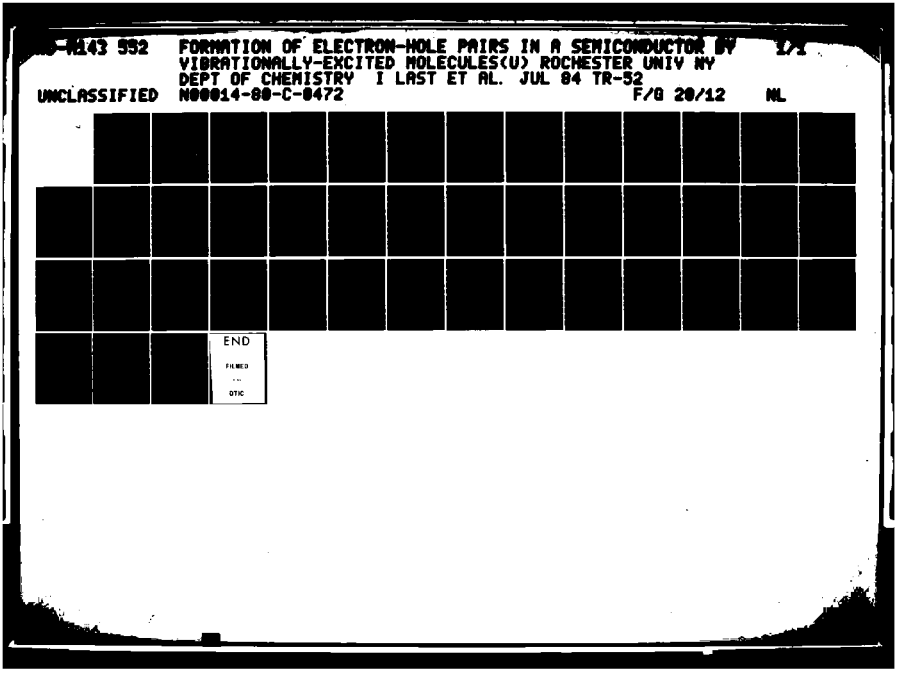
-A143 952
FORMATION OF ELECTRON-HOLE PAIRS IN A SEMICONDUCTOR BY
VIBRATIONALLY-EXCITED MOLECULES(U) ROCHESTER UNIV NY
DEPT OF CHEMISTRY I LAST ET AL. JUL 84 TR-52
UNCLASSIFIED N00014-80-C-0472
F/G 20/12
NL
END
FILMED
DTIC

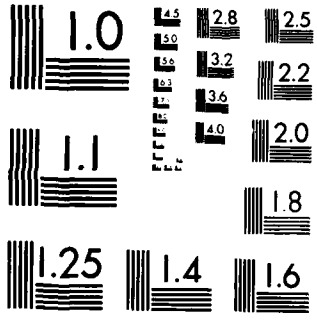

MICROCOPY RESOLUTION TEST CHART
NATIONAL BUREAU OF STANDARDS-1963-A

(12)

OFFICE OF NAVAL RESEARCH

Contract N00014-80-C-0472

Task No. NR 056-749

TECHNICAL REPORT No. 52

AD-A143 552

Formation of Electron-Hole Pairs in a Semiconductor by Vibrationally-Excited Molecules

by

Isidore Last and Thomas F. George

Prepared for Publication

in

Langmuir

Department of Chemistry
University of Rochester
Rochester, New York 14627

July 1984

Unclassified

SECURITY CLASSIFICATION OF THIS PAGE (When Data Entered)

REPORT DOCUMENTATION PAGE	READ INSTRUCTIONS BEFORE COMPLETING FORM
1. REPORT NUMBER: 52	2. GOVT ACCESSION NO.: AD-A143 552
	3. RECIPIENT'S CATALOG NUMBER:
4. TITLE (and Subtitle): Formation of Electron-Hole Pairs in a Semiconductor by Vibrationally-Excited Molecules	5. TYPE OF REPORT & PERIOD COVERED:
	6. PERFORMING ORG. REPORT NUMBER:
7. AUTHOR(s): Isidore Last and Thomas F. George	8. CONTRACT OR GRANT NUMBER(s): N00014-80-C-0472
9. PERFORMING ORGANIZATION NAME AND ADDRESS: Department of Chemistry, University ofRochester, Rochester, New York 14627	10. PROGRAM ELEMENT, PROJECT, TASK AREA & WORK UNIT NUMBERS: NR 056-749
11. CONTROLLING OFFICE NAME AND ADDRESS: Office of Naval Research, Chemistry Program Code 472, Arlington, Virginia 22217	12. REPORT DATE: July 1984
	13. NUMBER OF PAGES: 37
14. MONITORING AGENCY NAME & ADDRESS(if different from Controlling Office)	15. SECURITY CLASS. (of this report): Unclassified
	15a. DECLASSIFICATION/DOWNGRADING SCHEDULE:

16. DISTRIBUTION STATEMENT (of this Report)

This document has been approved for public release and sale; its distribution is unlimited.

17. DISTRIBUTION STATEMENT (of the abstract entered in Block 20, if different from Report)

18. SUPPLEMENTARY NOTES

Prepared for publication in Langmuir

19. KEY WORDS (Continue on reverse side if necessary and identify by block number)

CONDUCTIVITY	THEORETICAL STUDY
SEMICONDUCTORS	GOLDEN RULE EXPRESSION
GAS-SOLID INTERFACE	THREE-DIMENSIONAL MODEL
ENERGY TRANSFER	HCl + InSb & HCl + PbSe SYSTEMS
VIBRATIONAL-TO-ELECTRONIC	TRANSITION PROBABILITIES FROM 0.1 to 10 PERCENT

20. ABSTRACT (Continue on reverse side if necessary and identify by block number)

Both one-dimensional and three dimensional models are presented for the collision of a vibrationally-excited molecule sith a semiconductor surface, where the transfer of vibrational energy leads to the formation of electron-hole pairs. The transition probability P is calculated as a function of the molecule-surface distance for real two systems, HCl + InSb and HCl + PbSe, as well as for some model systems with different values of parameters. While P generally increases as the distance decreases, there are some maxima at intermediate distances. The overall probability is obtained as an approximate integral of P over the distance, and for thermal collisions values of

DD FORM 1 JAN 73 1473

Unclassified

SECURITY CLASSIFICATION OF THIS PAGE (When Data Entered)

a few percent are obtained. Such values are high enough for an experimental observation of electrical conductivity due to electron-hole pair formation.

LANGMUIR, *in press*

FORMATION OF ELECTRON-HOLE PAIRS IN A SEMICONDUCTOR BY VIBRATIONALLY-EXCITED MOLECULES

Isidore Last
Applied Mathematics
Soreq Nuclear Research Center
Yavne, 70600 ISRAEL

Thomas F. George
Department of Chemistry
University of Rochester
Rochester, New York 14627 USA

Abstract

Both one-dimensional and three-dimensional models are presented for the collision of a vibrationally-excited molecule with a semiconductor surface, where the transfer of vibrational energy leads to the formation of electron-hole pairs. The transition probability P is calculated as a function of the molecule-surface distance for real two systems, HCl + InSb and HCl + PbSe, as well as for some model systems with different values of parameters. While P generally increases as the distance decreases, there are some minima at intermediate distances. The overall probability is obtained as an approximate integral of P over the distance, and for thermal collisions values of a few percent are obtained. Such values are high enough for an experimental observation of electrical conductivity due to electron-hole pair formation.

I. Introduction

A vibrationally-excited molecule near a solid surface can transfer vibrational energy to either phonons or electrons (or both) of the solid. The situation involving excitation of phonons has been actively studied,[1-3] and theoretical investigations of energy transfer to the electrons of a solid have been carried out for the case of a metallic surface.[4-8] In the present study we consider the transfer of vibrational energy to the electrons of a semiconductor surface. This process differs from the case of a metallic surface due to the energy gap between the valence and conduction bands. Here the transfer of vibrational energy can excite electrons from the valence to the conduction band and hence result in the formation of electron-hole pairs which can be detected by measuring the semiconductor electrical conductivity.[9,10] In Section II we present a one-dimensional model which depends on a transition matrix element. This element is evaluated in Section III, and the results are used to determine the transition probability in Section IV. The polarization of the solid state is considered in Section V, and an extension to three dimensions is discussed in Section VI. The results of numerical calculations, with specific applications to the HCl + InSb and HCl + PbSe systems, are presented in Section VII, and Section VIII is the Summary and Concluding Remarks.

II. The Model

Let us consider a diatomic molecule whose center of mass is located at some distance R from a semiconductor surface. Within the framework of a one-dimensional model, the molecule is assumed to be oriented perpendicular to the surface on the continuation of a line formed by a linear chain of lattice atoms (Fig. 1), where the interaction of the molecule with the solid is restricted to just the atoms on the chain. We assume the velocity of the molecule to be sufficiently low such that the influence of its translational motion can be neglected. While the vibrational motion of the molecule affects the motion of both the nuclei and electrons of the lattice, we shall consider its effect only on the electrons.

The transfer of molecular vibrational energy to the chain electrons leads to the excitation of electrons from the valence band to the conduction band and therefore to the formation of electron-hole pairs. Such excitation is possible only when the vibrational energy level spacing $E_v = \hbar\omega$ is larger than the semiconductor band gap energy E_g (Fig. 2),

$$E_v = \hbar\omega > E_g. \tag{1}$$

For simplicity we take the molecule to be in its first-excited vibrational state and assume the influence of the solid on its vibrational motion to be negligible so that E_v is constant. We further restrict ourselves to cases where E_v is less than $2E_g$ so that only a one-electron transition is possible.

Considering the coupling between the vibrational motion of the molecule and the solid electrons as a weak perturbation, we can use the golden rule to determine the transition probability, which can be written for the case of a one-electron transition between two continua as

$$P = \frac{2\pi}{\hbar}\int_{E_V^{min}}^{E_V^{max}} dE_V\, n_V(E_V)\, n_C(E_C)\, W_{01}^2(E_V, E_C). \tag{2}$$

P is the probability of transition per second, E_V and E_C are one-electron energies of the valence and conduction bands, respectively, n_V is the density of electron states in the valence band, n_C is the density of empty levels in the conduction band, and W_{01} is the matrix element for the transition from the excited vibrational state to the ground state with a simultaneous transition from the valence band to the conduction band. Due to energy conversation, for this transition the E_C level is greater than E_V by the vibrational quantum E_v,

$$E_C = E_V + E_v \quad . \tag{3}$$

The upper limit on the integral is the maximum electronic level of the valence band, and the lower limit is given by

$$E_V^{min} = E_V^{max} - (E_v - E_g) \quad . \tag{4}$$

The matrix element W_{01} is expressed as an integral over the electronic coordinate z and the vibrational coordinate Z (Fig. 2),

$$W_{01}(E_V, E_V+E_g) = \int dz dZ \; \psi^{(V)}_{E_V}(z) \; \chi_1(Z) \hat{W}(z,Z) \psi^{(C)}_{E_V+E_v}(z) \chi_0(Z), \tag{5}$$

where $\psi^{(V)}$ and $\psi^{(C)}$ are the electronic warefunctions in the valence and conduction bands, respectively, χ_0 and χ_1 are the ground and first-excited state vibrational warefunctions, respectively, and $\hat{W}$ is the interaction between the electron and the molecule. At close distances, where the overlap between the molecular orbitals and the electronic states of the solid cannot be neglected, $\hat{W}$ is complicated. At far enough distances where the overlap can be neglected, $\hat{W}$ becomes electrostatic. If the size of the molecule is smaller than the distance to the solid-state electron, then the field of the vibrating molecule can be expressed as a sum of dipole and higher-order multipole potentials. We shall consider only the point dipole potential,

as has been done for the case of a metal surface.[6] If the polarization of the solid is neglected, i.e., setting the dielectric constant equal to one, then the interaction becomes (in atomic units).

$$\hat{W} = \frac{p(Z)}{(R-z)^2} \quad , \tag{6}$$

where p(Z) is the dipole moment. Substituting Eq. (6) into (5), we obtain a separation of variables.

$$W_{01}(E_V, E_V+E_v) = p_{01} \int_{-L}^{\infty} dz \; \psi_{E_V}^{(V)}(z) \; \frac{1}{(R-z)^2} \; \psi_{E_V+E_v}^{(C)}(z) \quad , \tag{7}$$

where L is the length of the chain and p_{01} is the dynamic dipole moment for the $1 \rightarrow 0$ transition,

$$p_{01} = \int_{-\infty}^{\infty} dZ \; \chi_0(Z) p(Z) \chi_1(Z) \quad . \tag{8}$$

The separation of variables is also achievable when other multipole moments are included in $\hat{W}$. The dynamic dipole moment is known for many diatomic molecules from experiments and/or <u>ab initio</u> calculations. The determination of W_{01} is thus reduced to the evaluation of a one-dimensional integral over the solid-state electronic coordinate. In the model considered here, only polar molecules can transfer vibrational energy to the solid. However, at close distances, particularly for an adsorbed molecule, this transfer is possible also for non-polar molecules due to the overlap between the molecular orbitals and the electronic states of the solid.

III. Transition Matrix Element

In order to calculate the transition matrix element displayed in Eq. (7), one must know the solid-state electronic wavefunctions $\psi^{(V)}$ and $\psi^{(C)}$. Forms for these are available in terms of the wavenumber k,[11,12] but we can reexpress these in unitless and more symmetrical forms in terms of the parameter x determined from the equations

$$k = \frac{g}{2}(1+x), \qquad -1 \leq x \leq 1 \tag{9}$$

$$x = \frac{2n}{N} - 1 = \frac{2a}{L} n - 1, \tag{10}$$

where $g = Nk/n = 2\pi/a$ is the reciprocal lattice constant, a is the lattice constant, n is an integer ($0 \geq n \geq N$), and $N = L/a$ is the number of unit cells. The wavefunctions and also the energies then can be written as

$$\psi_x^{(V)}(u) = \frac{1}{\sqrt{2\gamma}}\left[\sqrt{\gamma-x}\ \ \phi_x^{(V)}(u) + \sqrt{\gamma+x}\ \phi_{-x}^{(V)}(u)\right] \tag{11}$$

$$\psi_x^{(C)}(u) = \frac{1}{\sqrt{2\gamma}}\left[\sqrt{\gamma+x}\ \ \phi_x^{(C)}(u) + \sqrt{\gamma-x}\ \phi_{-x}^{(C)}(u)\right] \tag{12}$$

$$\phi_x^{(V)}(x) = \begin{cases} \sqrt{2}\ \sin[\pi(1+x)(u-u_d) + \theta_x], & u \leq u_d \qquad (13) \\ \sqrt{2}\ \sin\theta_x \exp[-\pi\sqrt{8\Gamma-(1+x)^2}(u-u_d)], & u > u_d \qquad (14) \end{cases}$$

$$E_V(x) = \frac{g^2}{8}\left[1+x^2 - 2\sqrt{4\zeta^2+x^2}\right] \tag{15}$$

$$\phi_x^{(C)}(u) = \begin{cases} -\sqrt{2}\ \cos\left[\pi(1+x)(u-u_d) + \theta_x\right], & u > u_d \qquad (16) \\ -\sqrt{2}\ \cos\theta_x \exp\left[-\pi\sqrt{8\Gamma-(1+x)^2}(u-u_d)\right], & u \leq u_d \qquad (17) \end{cases}$$

$$E_C^{(x)} = \frac{g^2}{8}\left[1+x^2+2\sqrt{4\zeta^2+x^2}\right], \tag{18}$$

where $u = z/a$, $u_d = d/a$, d is a distance on the order of an atomic radius (an actual value is set in Section VII), $\zeta = E_g/g^2$, $\Gamma = W/g^2$, W is the sum of the work function and Fermi energy, $\gamma = \sqrt{4\zeta^2+x^2}$, and

$$\tan\theta_x = (1+x)/\sqrt{8\Gamma-(1+x)^2}. \tag{19}$$

The wavefunctions $\phi^{(V)}$ and $\phi^{(C)}$ are normalized to the unit length.

Substituting the above forms of the wavefunctions into the integral of Eq. (7) and extending the lower limit of integration to $-\infty$, we obtain for arbitrary $\psi_x^{(V)}$ and $\psi_{\tilde{x}}^{(C)}$:

$$W_{01} = \frac{P_{01}}{a} Q(x,\tilde{x}) \tag{20}$$

$$Q(x,\tilde{x}) = \frac{1}{2\sqrt{\gamma\tilde{\gamma}}}\left[\sqrt{(\gamma-x)(\tilde{\gamma}+x)}\, S_{x,\tilde{x}} + \sqrt{(\gamma-x)(\tilde{\gamma}-x)}\, S_{x,-\tilde{x}}\right. \tag{21}$$

$$\left. + \sqrt{(\gamma+x)(\tilde{\gamma}+x)}\, S_{-x,\tilde{x}} + \sqrt{(\gamma+x)(\tilde{\gamma}-x)}\, S_{-x,-\tilde{x}}\right]$$

$$S_{x,\tilde{x}} = S_{x,\tilde{x}}^{(I)} + S_{x,\tilde{x}}^{(II)} \tag{22}$$

$$S_{x,\tilde{x}}^{(I)} = -2\sin\theta_x\cos\theta_{\tilde{x}} \int_0^\infty dt\, \exp[-\pi(\sqrt{8\Gamma-(1+x)^2}$$

$$+ \sqrt{8\Gamma-(1+\tilde{x})^2})t] \quad \frac{1}{(\rho-t)^2}, \tag{23}$$

$$t = u-u_d$$

$$S_{x,\tilde{x}}^{(II)} = -2\int_0^\infty dt\, \Omega(t) \tag{24}$$

$$\Omega(t) = \sin[\pi(1+x)t - \theta_x]\cos[\pi(1+\tilde{x})t-\theta_x] \frac{1}{(\rho+t)^2}, \tag{25}$$

$$t = u_d-u$$

where $\rho = u_R - u_d$ and $u_R = R/a$.

The integral in Eq. (23), which describes the interaction with the decaying portions of the wavefunctions outside the solid--Eqs. (14) and (17), goes to infinity at $t = \rho$. However, for t close to ρ the point dipole approximation is not valid and the finite size of the molecule must be taken into account. Fortunately, the integral in Eq. (23) is usually smaller than the integral in Eq. (25) so that the former can be treated approximately. The finite size of the dipole can be accounted for by replacing the term $(\rho-t)^2$ by $(\rho-t)^2 + \rho_M^2$, where ρ_M is a distance on the order of the relative (per lattice constant a) size of the dipole (molecule) This procedure is valid only for $\rho > \rho_M$. Usually the exponential function in E (23) decreases quickly and becomes small when $t \gtrsim \rho_M$. Accounting for this b vior and taking ρ to be greater than ρ_M, we may neglect the t-dependence of the term $(\rho-t)^2 + \rho_M^2$ and express Eq. (23) roughly as

$$S^{(I)}_{x,x} = - \frac{2\sin\theta_x \cos\theta_{\tilde{x}}}{\pi(\sqrt{8\Gamma-(1+x)^2} + \sqrt{8\Gamma-(1+\tilde{x})^2})(\rho^2+\rho_M^2)} \quad . \tag{26}$$

The integral of Eq. (24) which describes the interaction with the bulk portions of the wavefunctions is expressed in terms of sine and cosine integrals as

$$S^{(II)}_{x,\tilde{x}} = -T^{(+)}_{x,\tilde{x}} - T^{(-)}_{x,\tilde{x}} \tag{27}$$

$$T^{(+)}_{x,\tilde{x}} = \frac{1}{\rho}\sin(\theta_x+\theta_{\tilde{x}}) + \pi(2+x+\tilde{x})\, U^{(+)}_{x,\tilde{x}} \tag{28}$$

$$T^{(-)}_{x,\tilde{x}} = \frac{1}{\rho}\sin(\theta_x-\theta_{\tilde{x}}) + \pi(x-\tilde{x})\, U^{(-)}_{x,\tilde{x}} \tag{29}$$

$$U^{(+)}_{x,\tilde{x}} = \cos(\pi\alpha+\theta_x+\theta_{\tilde{x}})\mathrm{ci}(\pi\alpha) + \sin(\pi\alpha+\theta_x+\theta_{\tilde{x}})\mathrm{si}(\pi\alpha) \tag{30}$$

$$U^{(-)}_{x,\tilde{x}} = \cos(\pi\beta+\theta_x-\theta_{\tilde{x}})ci(\pi\beta) + \sin(\pi\beta+\theta_x-\theta_{\tilde{x}})si(\pi\beta) \quad , \tag{31}$$

where $\alpha = (2+x+\tilde{x})_\rho$ and $\beta = (x-\tilde{x})_\rho$.

IV. Transition Probability

The transition probability can be calculated according to Eq. (2) by integrating over the electron energy. However, it is more convenient to perform the integration in terms of the variable x which determines the wavenumber as in Eq. (9). The integration must be performed from $-x_0$ to $+x_0$, where x_0 corresponds to the energy E_V^{min}, also taking into account that for each x there are two transitions: $x \to \tilde{x}$ and $x \to -\tilde{x}$ with transition energy equal to the vibrational energy E_v (Fig. 3). Due to the symmetry of signs in Eq. (21) -- $Q(x,\tilde{x}) = Q(x,-\tilde{x}) = Q(-x,\tilde{x}) = Q(-x,-\tilde{x})$, we can change the lower integration limit to 0 simply by multiplying the integral in Eq. (2) by 4. Substituting Eq. (21) into (2), we then have

$$P = \frac{8\pi}{\tau_0}\left(\frac{p_{01}}{a}\right)^2 \int_0^{x_0} dx_V \left|\frac{dE}{dx_V}\right| n_V(x_V) n_C(x_C) Q^2(x_V,x_C), \tag{32}$$

where x_V corresponds to the energy E_V of the valence band and x_C to the energy $E_C = E_V + E_v$ of the conduction band and $\tau_0 = \hbar^3/m_e e^4 = 2.419\times10^{-17}$sec is a time atomic unit which has been inserted so that the quantities in the above equation can be expressed in atomic units, giving P in sec^{-1}.

Each level of the valence band is occupied by two electrons of opposite spin, so that n_V is obtained by doubling the level density, and n_C is simply equal to the level density due to conservation of spin in the band-to-band transition:

$$n_V(x_V) = 2\frac{dn_V}{dE_V} = \frac{1}{a}\left|\frac{dx_V}{dE_V}\right| \tag{33}$$

$$n_C(x_C) = \frac{dn_C}{dE_C} = \frac{1}{2a}\left|\frac{dx_C}{dE_C}\right| \quad , \tag{34}$$

where n_V and n_C are the numbers of levels with the wavenumber value $\leq \frac{q}{2}(1+x_V)$. Eq. (10) has been used to obtain $dn/dx = L/2a = 1/2a$, where the same normalization is used for the level densities as for the wavefunctions in Eqs. (13), (14), (16)

and (17) which were normalized to the unit length.

Combining the derivative of Eq. (18) with Eqs. (32)-(34), one can write

$$P = \frac{4A}{\pi\tau_0}\left(\frac{p_{01}}{a}\right)^2 f(u_R) \tag{35}$$

$$f(u_R) = \int_0^{x_0} dx_V \, Q^2(x_V, x_C) \, \frac{\sqrt{4\zeta^2+x_C^2}}{x_C(\sqrt{4\zeta^2+x_C^2}-1)} \tag{36}$$

where

$$x_0 = \sqrt{2}\left\{[1-2\zeta(2\xi-1)] - \sqrt{1-4\zeta(2\xi-1) + 4\zeta^2}\right\}^{\frac{1}{2}} \tag{37}$$

$$x_C = \left\{[2+8\xi\zeta-2\gamma+x_V^2] - 2\sqrt{1+4\zeta^2+8\xi\zeta-2\gamma+x_V^2}\right\}^{\frac{1}{2}} , \tag{38}$$

$\xi = E_v/E_g > 1$, and ζ and γ are defined just after Eq. (18). At the point $x_V = x_0$, x_C equals zero but the integral is finite, because in the vicinity of $x_V = x_0$ the variable x_C is proportional to $\sqrt{x_0 - x_V}$. The integral must be evaluated numerically.

We should mention that the transition probability can also be expressed directly as an integral over energy as follows:

$$f(u_R) = \int_{E_1}^{E_2} dE \, \frac{1}{y_V y_C} \left| 1 - \frac{1}{\sqrt{4\zeta^2+E}} \right| \left| 1 - \frac{1}{\sqrt{4\zeta^2+8\xi\zeta+E}} \right| \tag{39}$$

where $E = 8E_V/g^2$, $E_1 = 1-4\zeta(2\xi-1)$, $E_2 = 1-4\zeta$, and

$$y_V = \left| 2\sqrt{4\zeta^2+u} - 1 - u \right|^{\frac{1}{2}} \tag{40}$$

$$y_C = \left| 2\sqrt{4\zeta^2+8\xi\zeta+u} - 1 - u - 8\xi\zeta \right|^{\frac{1}{2}} . \tag{41}$$

V. Polarization of the Solid State

The expression for the transition matrix element in Eq. (20) was obtained by the assumption that the electrical field [Eq. (6)] in the bulk is the same as in the vacuum. In other words, the dielectric constant ε, which is often large for semiconductors, was set equal to one. The dielectric constant cannot be taken into account simply by introducing it into the interaction in Eq. (6). In the vicinity of the surface the dielectric constant is a function of the distance from the surface, changing from 1 outside the solid to ε deep inside the solid. It is just this region at the surface which is the most important for the transition matrix element of Eq. (20). Unfortunately, the introduction of any reasonably smooth function $\varepsilon'(z)$ into the integral of Eq. (24) precludes an analytical solution. The simplest way to account for the polarization of the solid is to make $\varepsilon'(z)$ a step function,

$$\varepsilon'(z) = \begin{cases} 1, & z \geq -b \\ \varepsilon, & z < -b \end{cases} , \tag{42}$$

where the parameter b is expected to be on the order of the diameter of the Onsager cavity, which can be assumed to be the diameter of an atom.[13] Introducing this into Eq. (24), we obtain

$$S^{(II)}_{x,\tilde{x}} = -\frac{2}{\varepsilon}\int_{u_d+u_b}^{\infty} du\,\Omega(u) - 2\int_{0}^{u_d+u_b} du\,\Omega(u) , \tag{43}$$

where $\Omega(u)$ is the function of Eq. (25) and $u_b = b/a$. Evaluating the above two integrals in the same way as for Eq. (24), we obtain

$$S^{(II)}_{x,\tilde{x}} = -T^{(+)}_{x,\tilde{x}} - T^{(-)}_{x,\tilde{x}} + \frac{\varepsilon-1}{\varepsilon}\left[F^{(+)}_{x,\tilde{x}} + F^{(-)}_{x,\tilde{x}}\right] , \tag{44}$$

where the first two terms on the right-hand side are given by Eqs. (28) and (29).

The last two terms are:

$$F^{(+)}_{x,\tilde{x}} = \frac{1}{\rho_b}\sin[\theta_x + \theta_{\tilde{x}} - \pi(\alpha_b-\alpha)] + \pi(2+x+\tilde{x})G^{(+)}_{x,\tilde{x}} \tag{45}$$

$$F^{(-)}_{x,\tilde{x}} = \frac{1}{\rho_b}\sin[\theta_x - \theta_{\tilde{x}} - \pi(\beta_b-\beta)] + \pi(x-\tilde{x})G^{(-)}_{x,\tilde{x}} \tag{46}$$

$$G^{(+)}_{x,\tilde{x}} = \cos(\pi\alpha + \theta_x + \theta_{\tilde{x}})\,ci(\pi\alpha_b) + \sin(\pi\alpha + \theta_x + \theta_{\tilde{x}})\,si(\pi\alpha_b) \tag{47}$$

$$G^{(-)}_{x,\tilde{x}} = \cos(\pi\beta + \theta_x - \theta_{\tilde{x}})\,ci(\pi\beta_b) + \sin(\pi\beta + \theta_x - \theta_{\tilde{x}})\,si(\pi\beta_b)\ , \tag{48}$$

where $\alpha_b = (2 + x + \tilde{x})u_b$, $\beta_b = (x - \tilde{x})u_b$ and $\rho_b = u_R + u_b$.

VI. Three Dimensions

The vibrationally-excited molecule can obviously form electron-hole pairs not only in the chain on the same line with the molecule (Fig. 1) but also in other chains and in different directions of the electron motion. The consideration of this three-dimensional interaction is very complicated, and in order to simplify the problem we shall introduce some assumptions which enable us to reduce the three-dimensional integration to an integration over the surface.

The solid state is envisioned as formed by a series of one-dimensional chains which are parallel to each other and perpendicular to the surface. The interaction between the molecule and a chain which is not on the same line as the molecule is assumed to be determined by the expression for the one-dimensional case, taking into account only the difference in the distance and the influence of the dipole orientation on the perpendicular component of the field at the surface point A (Fig. 4). Taking the lattice to be formed by two kinds of atoms with similar sizes and the distribution of atoms to be uniform, we can then express the transition probability as

$$P = \frac{4A}{\pi\tau_0}\left(\frac{p_{01}}{a}\right)^2 \left[f(u_R) + 8\pi\int_{0.5}^{\infty} du_r \frac{(2u_R^2-u_r^2)^2}{4u_A^4} u_r f(u_A)\right], \tag{49}$$

where $u_r = r/a$, $u_A = R_A/a = \sqrt{u_R^2 + u_r^2}$, and R_A is the distance between the dipole and the point A. The lower limit of integration is taken to be half of the lattice constant, considering it approximately as the distance from the point 0 to the closest neighboring atom. The factor $(2u_R^2 - u_r^2)^2/4u_A^4$ is equal to the square of the ratio between the z-component of the dipole field at the point A and the field in the one-dimensional case for the same distance from the dipole.

The above approximations better describe the interaction with the solid-state electrons which are close to the surface than with the electrons deep in the bulk. Fortunately, when the dielectric constant is large the electrons deep in the bulk

interact relatively weakly with the molecule and hence do not have a significant effect on the transition probability.

VII. Numerical Results

All results were obtained for a simple lattice of two kinds of atoms (Figs. 1 and 4), where the one-dimensional unit cell consists of two atoms only. With the assumption that the atoms do not differ much in their size, the parameter d [mentioned just after Eq. (18)] can be taken as equal to the average atomic radius, which is approximately a quarter of the lattice constant, i.e., a/4 (u_d = 0.25). The parameter b for the dielectric constant in Eq. (42) is assumed to be equal to the atomic diameter, a/2 (u_b = 0.5).

The transition probability given by Eq. (35) is proportional to the square of the ratio p_{01}/a, where p_{01} is the dynamic dipole moment of the molecule for the $1 \rightarrow 0$ vibrational transition. The dependence on the molecule-surface distance as well as on other parameters is included in the function $f(u_R)$. This function depends on unitless quantities only, such as the relative molecule-surface dustance u_R [defined just after Eq. (25)], the relative energy gap ζ [after Eq. (18)], the sum W of the work function and Fermi energy, and the ratio ξ between the vibrational energy and the energy gap [after Eq. (38)]. The function $f(u_R)$ depends very weakly on the parameter Γ, which is determined by W [after Eq. (18)]. In all calculations we take Γ to be 0.7, which corresponds approximately to W = 5 eV for the semiconductor InSb.

In order to investigate the behavior of the transition probability on u_R as determined by $f(u_R)$, we have carried out calculations for different values of the parameters ζ and ξ and the dielectric constant ε. All results, except for the one case of the HCl + PbSe system, are presented for the lattice constant of the semiconductor InSb, a = 6.48 Å (12.24 a.u.),[14] and the dynamic dipole moment of the HCl molecule, p_{01} = 0.0712 D (0.0279 a.u.).[15] The results for other values of p_{01} and a can be obtained simply from the equation

$$\tilde{P}(u_R;\zeta,\xi,\varepsilon) = \left(\frac{\tilde{p}_{01}}{0.0712}\right)^2 \left(\frac{6.48}{\tilde{a}}\right)^2 P(u_R;\zeta,\xi,\varepsilon), \tag{50}$$

where $\tilde{p}_{01}$ and $\tilde{a}$ are expressed in the units D and Å, respectively.

Results for the dielectric constant $\varepsilon = 1$ are presented in Fib. 5. The most interesting feature of the curves is that the transition probability P does not decrease monotically as the molecule-surface distance increases. The curves (dashed lines) for the one-dimensional (1D) calculation exhibit a deep minimum which is shifted toward the surface as the vibrational energy decreases, i.e., as ξ decreases. In the three-dimensional (3D) calculation, the curves (solid lines) are smoother, as might be expected due to a "smearing-out" effect, but also have a minimum which becomes very shallow for large vibrational energies ($\xi = 2.0$). At large distances the 1D transition probability has a sharp decrease approximately proportional to $1/R^n$ ($n = 2$-4). The decrease is slower in the 3D case, and in fact, the decrease for $\xi = 1.1$ does not occur until $u_R = 12$. [We note that the 3D results obtained by the integration over the surface in Eq. (49) are very approximate for $\varepsilon = 1$ when electrons deep in the bulk of the semiconductor play a significant role.] At small distances P increases quite sharply with little distinction between different parameters and models (1D and 3D). Very close to the surface, when the size of the molecule is comparable to its distance from the surface, the point dipole approximation does not work well. However, for a relative distance u_R as small as 0.5 in the HCl + InSb system, for example, the molecule is 3.3 Å from the surface, which is over 2.5 times as large as the size of the molecule and hence large enough for the point dipole approximation to be valid.

Results for the dielective constant $\varepsilon = 15$ are presented in Fig. 6. These curves are smoother than those for $\varepsilon = 1$, and for small vibrational energy ($\xi = 1.1$) they decrease monotonically as the distance increases. Except for very small distances, the transition probability is smaller and decreases more steeply at large distances for $\varepsilon = 15$ than for $\varepsilon = 1$. The influence of the dielectric constant on P is further demonstrated in Fig. 7, where results are presented for different ε but for the same values of the parameters ζ and ξ. While P decreases

at large distances as ε increases, the opposite behavior occurs in some intervals at intermediate distances.

The minimum in the transition probability at intermediate molecule-surface distances occurs because the contributions from different parts of the chain to the integrals of Eqs. (24) and (43) have different signs. This leads to an interference effect which is less important for large ε, where one unit cell of the chain, namely the closest to the surface, makes the main contribution to the integral.

The dependence of the transition probability on the molecule-surface distance for two real systems, HCl + InSb and HCl + PbSe, is presented in Fig. 8. In contrast to the results discussed earlier, the distance here is not in relative unitless numbers but rather in Å. The lattice parameters for the two semiconductors are similar -- a = 6.48 Å for InSb and a = 6.124 Å for PbSe.[14] The main differences are in the energy gap, which is larger for PbSe (0.26 eV) than for InSb (0.165 eV), and in the dielectric constant, which is much larger for PbSe (280) than for InSb (18).[16] At large distances P is much lower for PbSe mainly due to the larger value of ε, although at small and intermediate distances (4-21 Å) P is higher for PbSe.

It is possible to calculate the overall transition probability corresponding to each curve $P(u_R)$. If the molecule is moving with velocity v perpendicular to the surface, then this overall probability P_Σ is

$$P_\Sigma = \frac{a}{v} \int_{u_s}^{\infty} du\, P(u), \tag{51}$$

where $u = R/a$ and u_s is the minimal possible distance between the molecule and surface. It is reasonable to consider this to be the distance associated with an adsorbed molecule. However, the results obtained here cannot be continued to such short distances due to the approximations of the model. Nevertheless, we have

evaluated the above integral for values of u_s for which our model is valid, and P_Σ is given for three different values of u_s in Table I. The dependence of P_Σ on the parameters ε, ζ and ξ is presented in Table II for u_s = 0.5 and 0.9. In these calculations the 3D form of P(u) was used, and the HCl molecule was taken to be thermal (300 K) with a velocity $v = 4.0 \times 10^4$ cm/sec. We see that P_Σ is on the order of ten percent for u_s = 0.5 and is on the order of one percent for u_s as large as 0.9. For u_s=0.5 the probability does not depend as much on the dielectric constant, while for u_s= 0.9 it is much higher for ε = 1 than for ε = 15. It is interesting to note that as the vibrational energy parameter ξ increases, P_Σ decreases in spite of the increase in the number of band levels involved in the transition. This is due to the fact that for values of the parameter ξ close to 1, the transition takes place between levels whose spacing is close to the energy gap, so that the product of the level densities, $\eta_V\eta_C$, in the integral of Eq. (2) is large as η_V and η_C are going to infinity in the vicinity of the gap.

VIII. Summary and Concluding Remarks

For a vibrationally-excited molecule not very close to the semiconductor surface, the influence of the vibrational motion on the solid-state electrons can be taken as an electrostatic interaction with a point dipole. If the vibrational energy level spacing is larger than the semiconductor energy gap, this interaction leads to the excitation of electrons from the valence to the conduction band and hence to the formation of electron-hole pairs which can be detected by measuring the semiconductor electrical conductivity.

In the one-dimensional model the transition probability (per second) is expressed in terms of integrals of analytical functions which include such special functions as the sine and cosine integrals. Results from this model show the transition probability to increase sharply at short distances. At intermediate distances there is often a minimum followed by a maximum and then a further decrease of the probability. A three-dimensional calculation is performed approximately by the integration of a modified one-dimensional probability over the surface. In this case the probability is higher and the dependence on the molecule-surface distance is smoother than in the one-dimensional case. The overall probability of formation of an electron-hole pair, obtained by summing from the distance u_s to infinity, is on the order of ten percent when u_s is chosen to be 0.5 of the lattice constant a.

In an experimental situation, those molecules still excited at u_s will continue on toward the surface to undergo an elastic or inelastic encounter. Inelastic processes may involve either phonon or electron excitation or both. Because the events occurring after the molecule reaches u_s can only add to the probability of electron-hole formation, this theory provides a lower limit to the efficiency of that process. Experimentally,[17] efficiencies in the range 0.1 to 10% would be readily observable. In summary, this model calculation points out that vibrational-to-electronic energy transfer could be a significant energy

pathway at semiconductor surfaces. Possible applications include selective detection of vibrationally excited molecules.

Acknowledgments

This research was supported in part by the Air Force Office of Scientific Research (AFSC), United States Air Force, under Grant AFOSR-82-0046, and the Office of Naval Research. The United States Government is authorized to reproduce and distribute reprints for governmental purposes notwithstanding any copyright notation hereon. TFG acknowledges the Camille and Henry Dreyfus Foundation for a Teacher-Scholar Award (1975-84) and the John Simon Guggenheim Memorial Foundation for a Fellowship (1983-84). IL wishes to thank the University of Rochester for their hospitality during his visit in the Fall of 1983, when much of this research was carried out. Special thanks are given to Professor David S. Perry for suggesting this study. Finally, we want to acknowledge stimulating discussions with William C. Murphy.

References

1. G. Wolken, Jr., J. Chem. Phys. 60, 2210 (1976).
2. Y.-W. Lin and G. Wolken, Jr., J. Chem. Phys. 65, 2634 (1976); 65 3729 (1976).
3. A. C. Diebold and G. Wolken, Jr., Surface Sci. 82, 245 (1979).
4. L. E. Brus, J. Chem. Phys. 73, 940 (1980).
5. M. Perrson and B. N. J. Perrson, in Vibrations at Surfaces, ed. by R. Caudano, J. M. Gilles and A. A. Lucas (Plenum, New York, 1982), pp. 113-122.
6. B. N. J. Persson and N. D. Lang, Phys. Rev. B 26, 5409 (1982).
7. B. N. J. Perrson and W. L. Schaich, J. Phys. C: Solid State Phys. 14, 5583 (1981).
8. J. W. Gadzuk and H. Metiu, in Vibrations at Surfaces, ed. by R. Candano, J. M. Gilles and A. A. Lucas (Plenum, New York, 1982), pp. 519-540.
9. D. S. Perry, private communication.
10. I. Last, T. F. George and D. S. Perry, unpublished.
11. W. C. Murphy and T. F. George, Surface Sci. 114, 189 (1982).
12. T. F. George, J. Lin, A. C. Beri and W. C. Murphy, Prog. Surf. Sci., in press.
13. C. J. F. Böttcher, Theory of Electric Polarization. Vol. 1. Dielectrics in Static Fields (Elsevier, Amsterdam, 1973).
14. Handbook of Chemistry and Physics, 58th Ed. (CRC, West Palm Beach, Florida, 1977-78), Sec. E., pp. 101-103.
15. W. E. Kaiser, J. Chem. Phys. 53, 1686 (1970).
16. American Institute of Physics Handbook, 3rd Ed. (McGraw-Hill, New York, 1972), Sec. 9, p. 72.
17. The combination of pulsed molecular beams and pulsed lasers makes possible a flux of vibrationally-excited molecules of 10^{20} $sec^{-1}steredian^{-1}$ [see, for example, M. G. Liverman, S. M. Beck, D. L. Monts and R. E. Smalley, Rarefield Gas Dynamics 11 (2), 1037 (1979)]. Because InSb and ZnSe have been developed as infrared photoconductor detectors, their conductivity noise characteristics are favorable. Noise equivalent powers in the range 10^{-10} to 10^{-12} $WHz^{\frac{1}{2}}$ are typical [see, for example, E. H. Putley, J. Sci. Instr. 43, 857 (1966)]. Under these conditions, electron-hole pair creation probabilities as low as a few parts per million would be detectable.

Table I. The overall transition probability P_Σ (in percent) for the systems HCl + InSb and HCl + PbSe. The HCl molecule is moving perpendicular toward the surface with the velocity $v = 4.0 \times 10^4$ cm/sec from infinity to the point $u_s = R/a$.

Semiconductor	InSb			PbSe		
ε	18.			280.		
ζ	0.023			0.0324		
ξ	2.17			1.377		
u_s	0.5	0.7	0.9	0.5	0.7	0.9
R (Å)	3.24	4.54	5.83	3.06	4.29	5.51
P_Σ (%)	4.2	0.91	0.33	7.1	2.0	0.87

Table II. The same as Table I but for HCl + semiconductor with different values of the parameters ε, ζ and ξ. P_{Σ} (0.5) and P_{Σ} (0.9) are given in percent for $u_s = 0.5$ and $u_s = 0.9$, respectively.

ε	1.	15.	15.	15.	15.	15.	50.
ζ	0.05	0.025	0.05	0.05	0.05	0.10	0.05
ξ	1.4	1.1	1.1	1.4	2.0	1.1	1.4
P (0.5)	11.3	5.7	10.8	8.5	5.5	19.9	8.8
P (0.9)	5.5	0.83	1.5	0.72	0.51	2.5	0.83

Figure Captions

1. Location of the molecule with respect to the solid-state atoms in a one-dimensional chain; a -- lattice constant, R -- molecule-surface distance, d -- border distance for the wavefunctions of Eqs. (11) and (12).
2. Band structure of the semiconductor; Z -- vibrational coordinate, z -- electronic coordinate, E_V^{max} -- top level of the valence band; E_C^{min} -- bottom level of the conduction band; E_v -- vibrational energy level spacing; E_V & E_C -- levels involved in the transition.
3. Band energies of the one-dimensional chain for the PbSe semiconductor. For the valence and conduction bands E_V and E_C see Eqs. (15) and (18), and for the parameter x see Eqs. (9) and (10). The parameters of the chain are: a = 6.124 Å, E_g = 0.26 eV, ζ = 0.0324.
4. Three-dimensional model; O -- center, M -- molecule, R -- molecule-surface distance, r -- distance on the surface from O to atom A, R_A -- molecule-atom-A distance.
5. Dependence of the transition probability P (per second) on the relative molecule-surface distance u_R = R/a. The value of the dielectric constant ε is 1. The numbers on the curves indicate the ratio $\xi = E_v/E_g$ between the vibrational energy level spacing and the energy gap. The dashed lines represent the results of the 1D calculation, and the solid lines represent the results of the 3D calculation. (a) Relative energy gap $\zeta = E_g/g^2 = 0.025$ and (b) ζ = 0.10. [The small gaps at u_R = 5 for the 3D curves are because of a change in the integration stepsize used in the evaluation of the integral in Eq. (49).]
6. Same as for Fig. 5 but for ε = 15.

7. Dependence of the transition probability P (per second) on the relative molecule-surface distance u_R, where $\zeta = 0.05$, $\xi = 1.4$, and the numbers on the curves indicate the dielectric constant ε (see also the caption to Fig. 5).
8. Dependence of the transition probability P (per second) on the molecule-surface distance R for the systems HCl + InSb and HCl + PbSe. The vibrational energy level spacing is 0.358 eV. The parameters for HCl + InSb are: $\varepsilon = 18$, $a = 6.48$ Å, $E_g = 0.165$ eV, $\zeta = 0.023$, $\xi = 2.17$. The parameters for HCl + PbSe are: $\varepsilon = 280$, $a = 6.124$ Å, $E_g = 0.26$ eV, $\zeta = 0.0324$, $\xi = 1.277$.

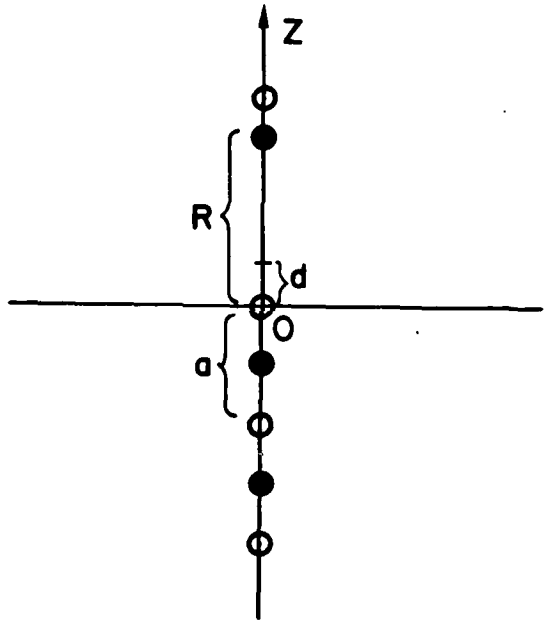

Fig 1

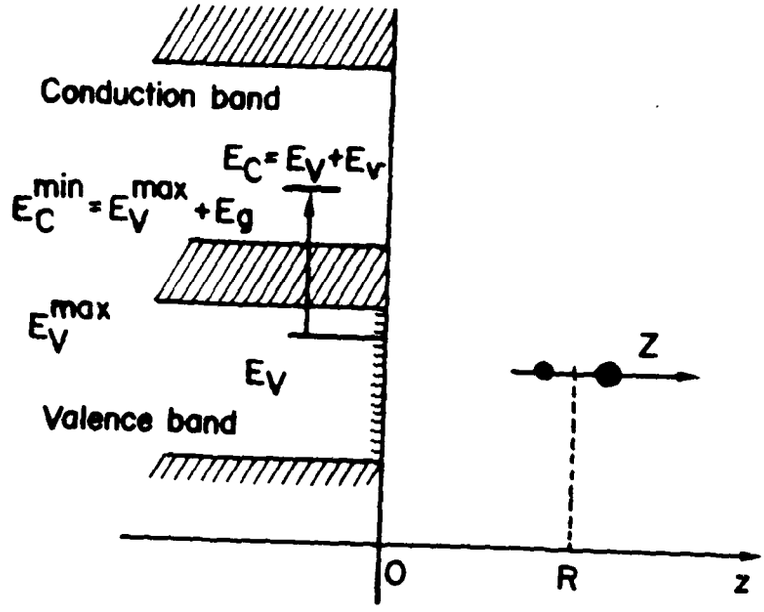
Conduction band
$E_C = E_V + E_v$
$E_C^{min} = E_V^{max} + E_g$
E_V^{max}
E_V
Valence band
Z
O
R
z

Fig. 2

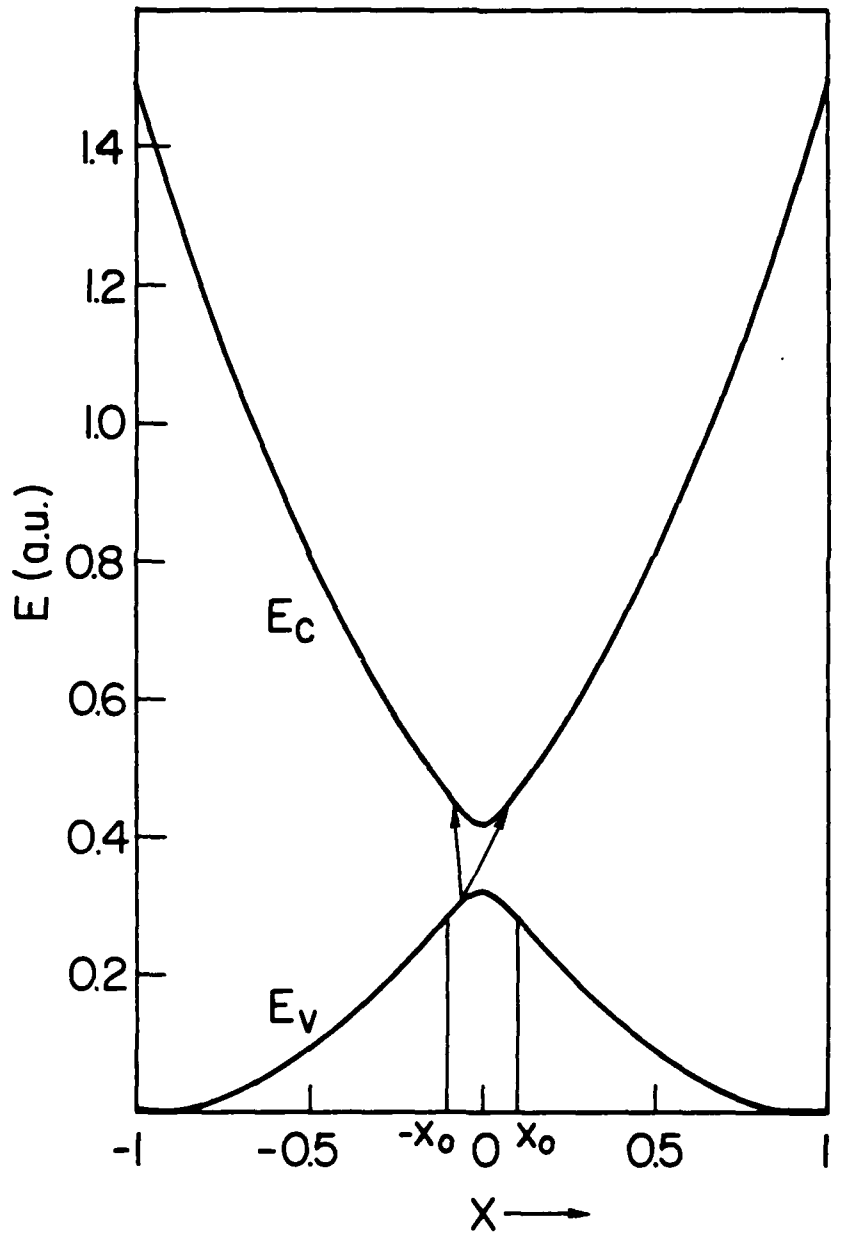

Fig 3

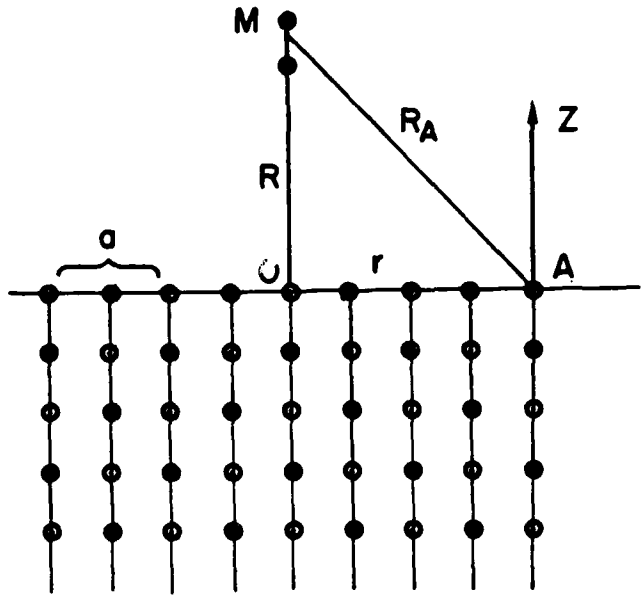

Fig. 4

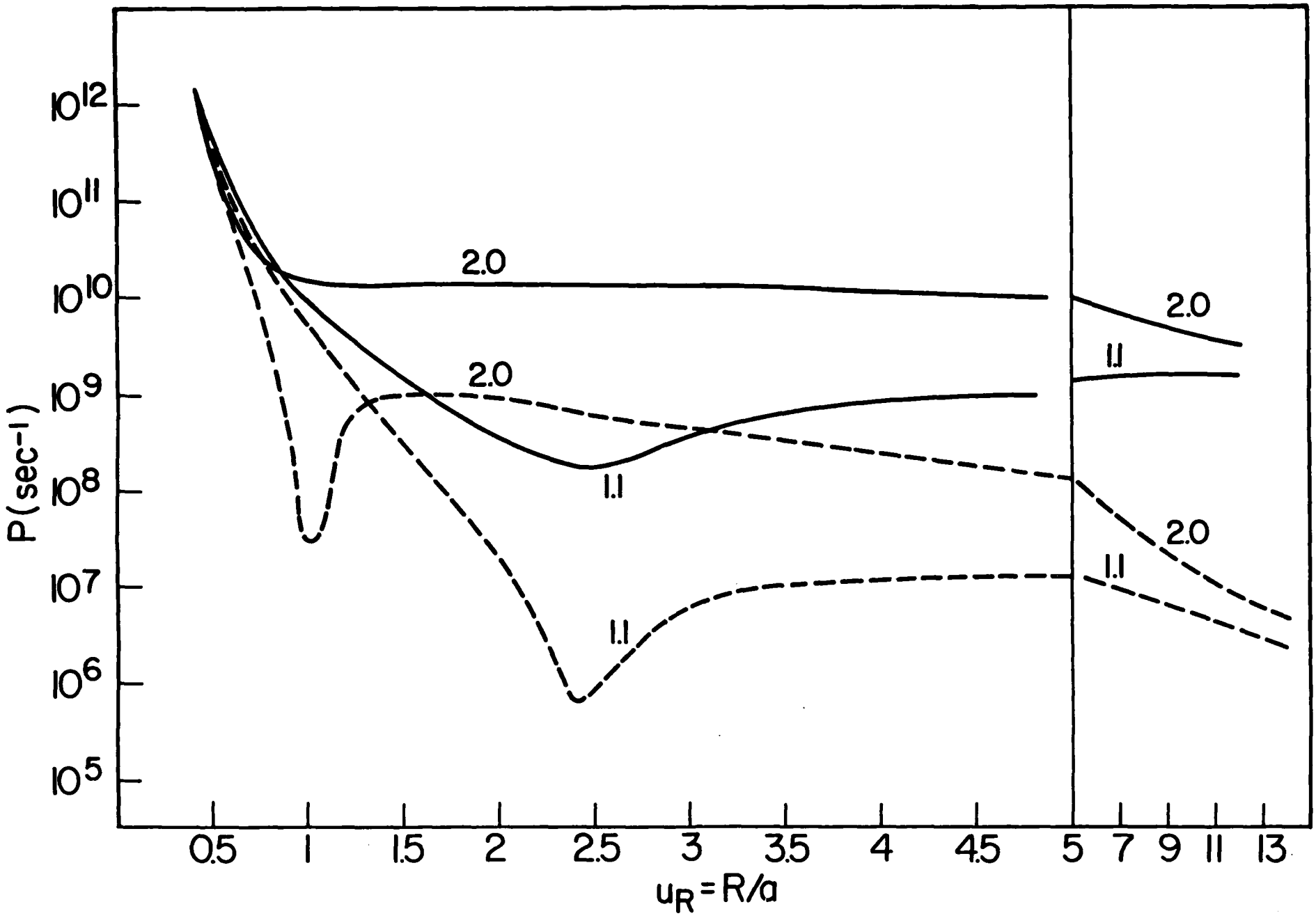
10^{12}
10^{11}
10^{10}
10^{9}
10^{8}
10^{7}
10^{6}
10^{5}
P(sec^{-1})
2.0
2.0
1.1
2.0
1.1
2.0
1.1
1.1
0.5
1
1.5
2
2.5
3
3.5
4
4.5
5
7
9
11
13
$u_R = R/a$

Fig. 5(a)

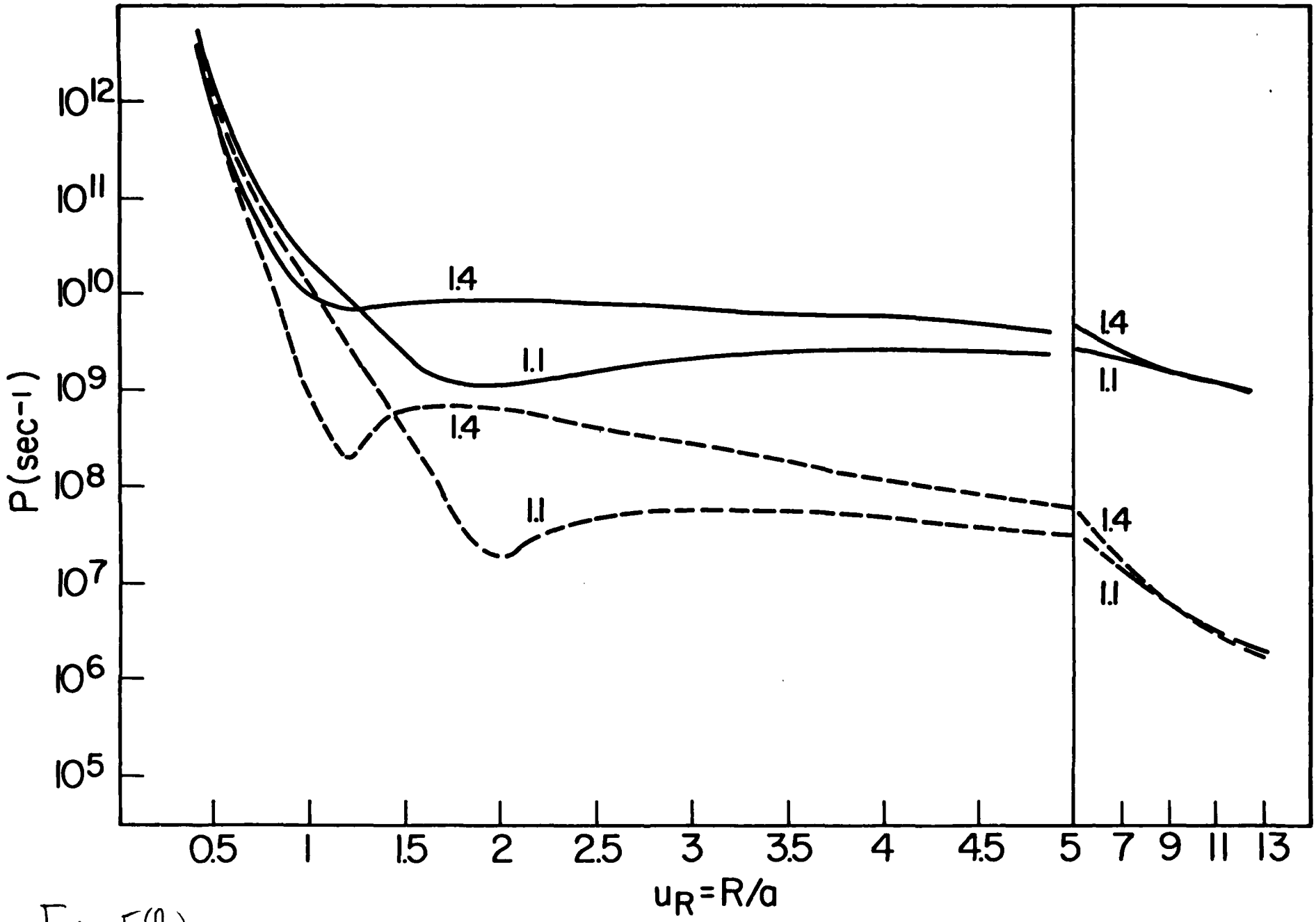
10^{12}
10^{11}
10^{10}
10^{9}
10^{8}
10^{7}
10^{6}
10^{5}
P(sec-1)
1.4
1.1
1.4
1.1
1.4
1.1
1.4
1.1
0.5
1
1.5
2
2.5
3
3.5
4
4.5
5
7
9
11
13
$u_R = R/a$

Fig. 5(b)

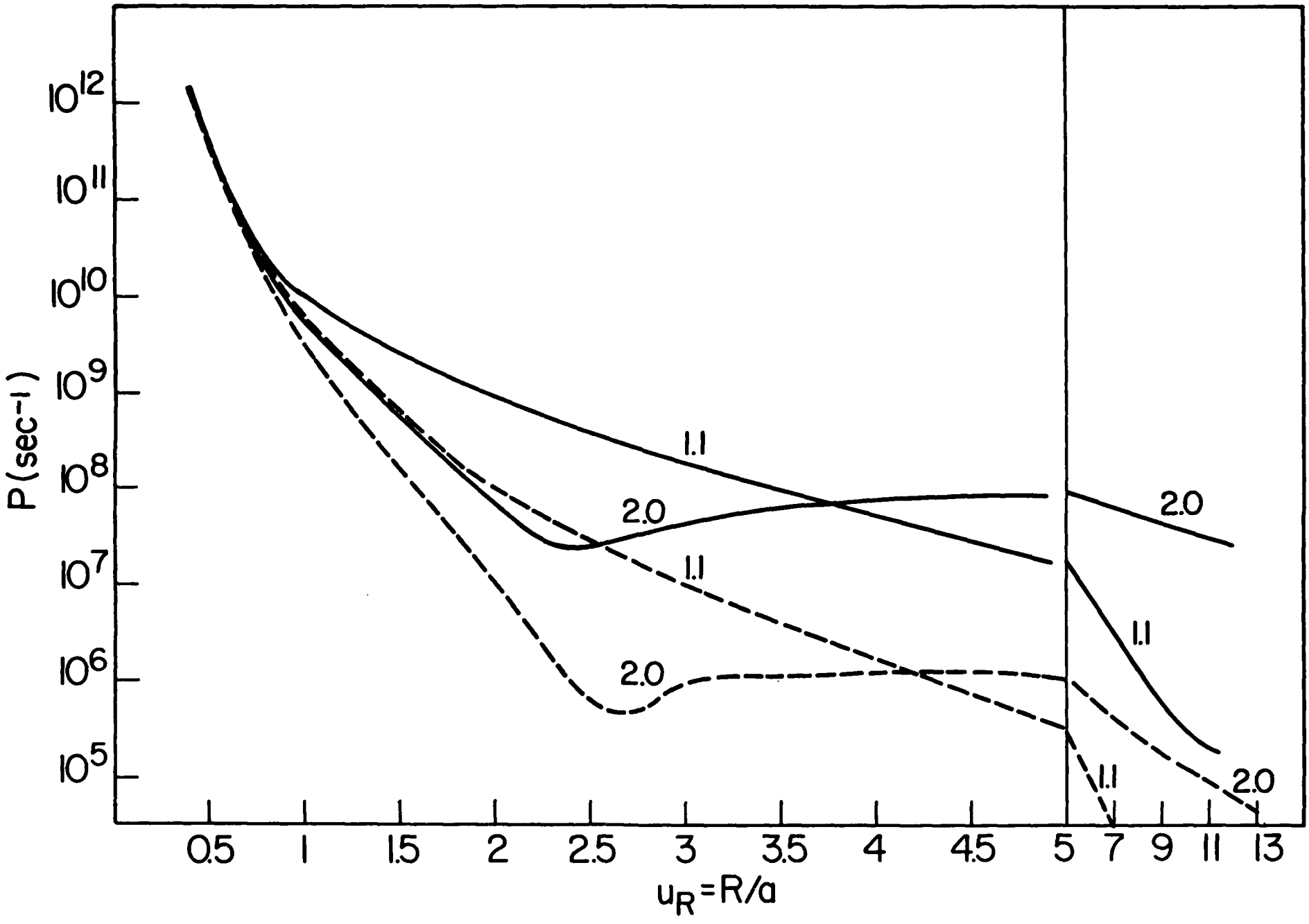
10^{12}
10^{11}
10^{10}
10^{9}
10^{8}
10^{7}
10^{6}
10^{5}
P(sec⁻¹)
1.1
2.0
1.1
2.0
1.1
2.0
1.1
2.0
0.5
1
1.5
2
2.5
3
3.5
4
4.5
5
7
9
11
13
$u_R = R/a$

Fig. 6(a)

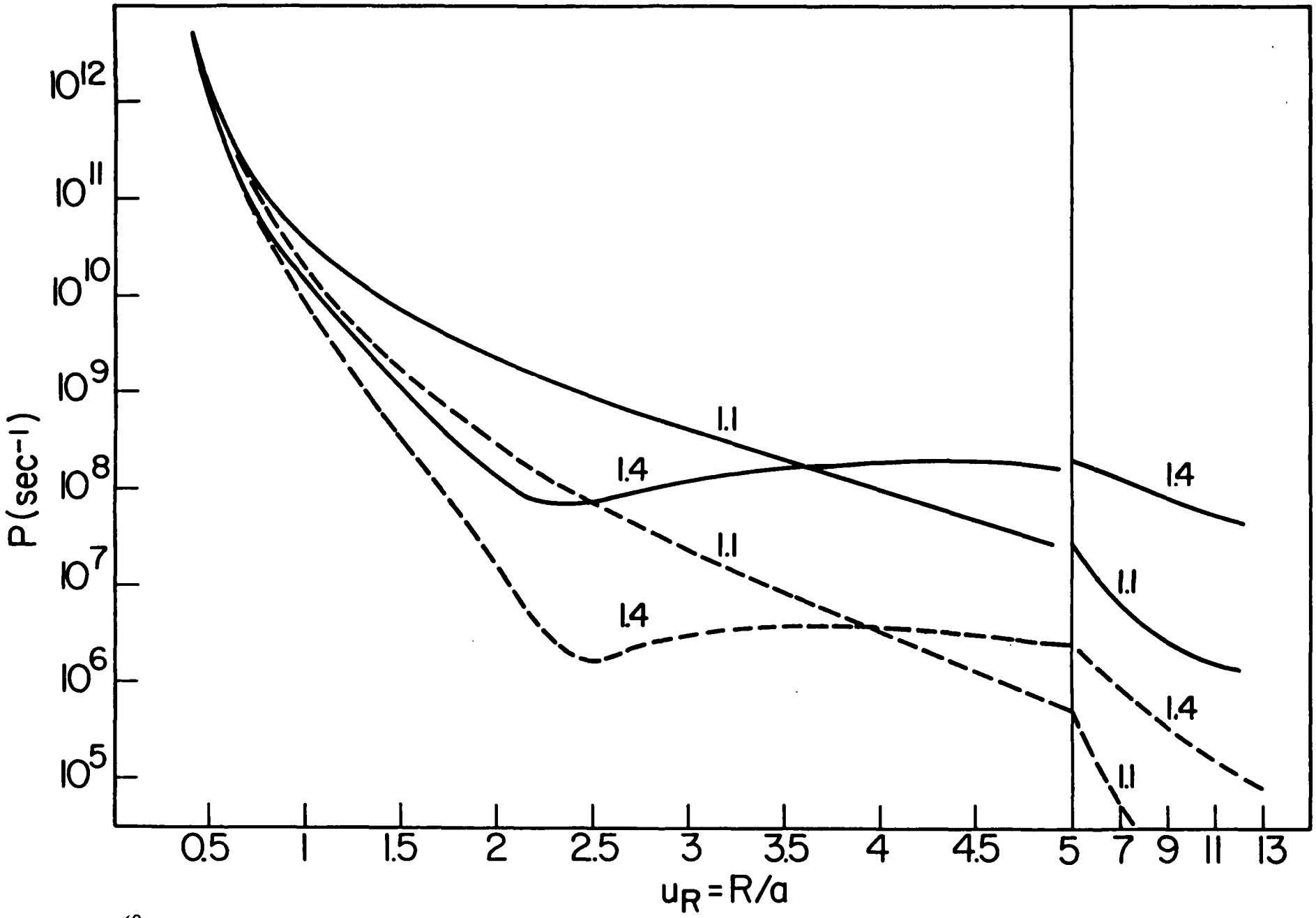
10^{12}
10^{11}
10^{10}
10^{9}
10^{8}
10^{7}
10^{6}
10^{5}
P(sec⁻¹)
1.1
1.4
1.1
1.4
1.4
1.1
1.1
1.4
1.1
0.5
1
1.5
2
2.5
3
3.5
4
4.5
5
7
9
11
13
$u_R = R/a$

Fig. 6(b)

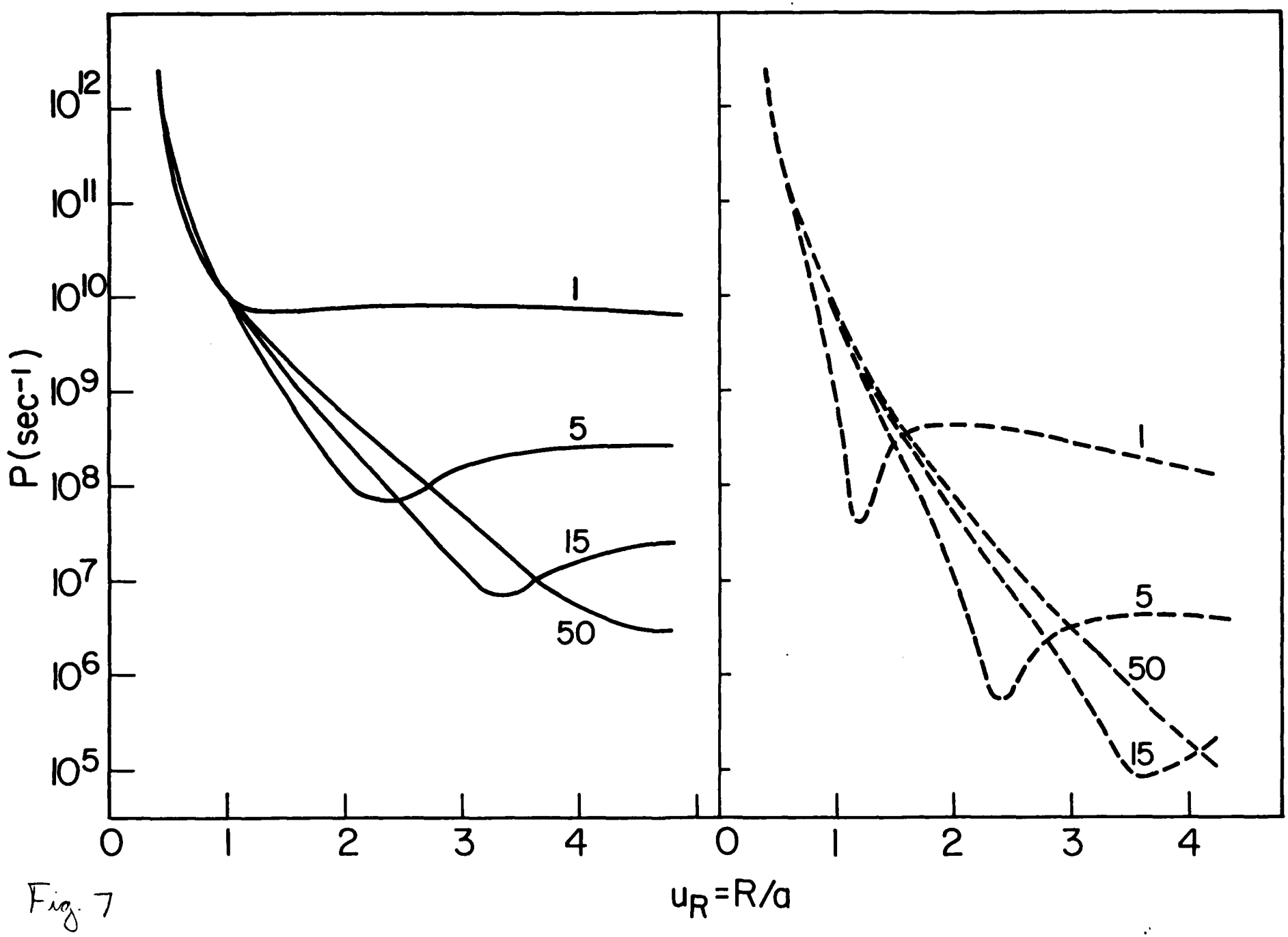
10^{12}
10^{11}
10^{10}
10^{9}
10^{8}
10^{7}
10^{6}
10^{5}
P(sec^{-1})
1
5
15
50
0
1
2
3
4
0
1
2
3
4
1
5
50
15
$u_R = R/a$

Fig. 7

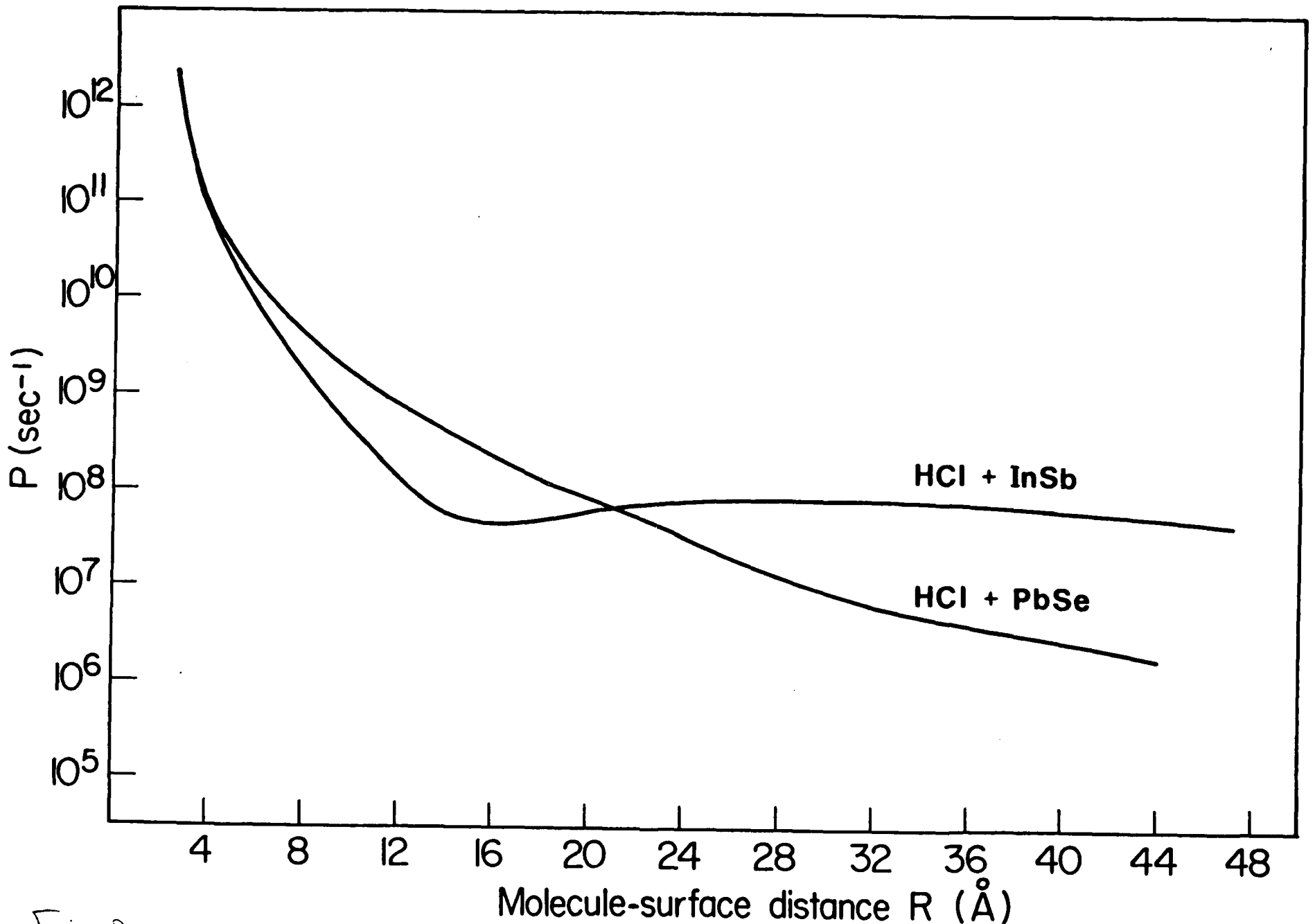
10^{12}
10^{11}
10^{10}
10^{9}
10^{8}
10^{7}
10^{6}
10^{5}
P (sec^{-1})
HCl + InSb
HCl + PbSe
4
8
12
16
20
24
28
32
36
40
44
48
Molecule-surface distance R (Å)

Fig. 8

DL/413/83/01
GEN/413-2

TECHNICAL REPORT DISTRIBUTION LIST, GEN

	No. Copies
Office of Naval Research Attn: Code 413 800 N. Quincy Street Arlington, Virginia 22217	2
ONR Pasadena Detachment Attn: Dr. R. J. Marcus 1030 East Green Street Pasadena, California 91106	1
Commander, Naval Air Systems Command Attn: Code 310C (H. Rosenwasser) Washington, D.C. 20360	1
Naval Civil Engineering Laboratory Attn: Dr. R. W. Drisko Port Hueneme, California 93401	1
Superintendent Chemistry Division, Code 6100 Naval Research Laboratory Washington, D.C. 20375	1
Defense Technical Information Center Building 5, Cameron Station Alexandria, Virginia 22314	12
DTNSRDC Attn: Dr. G. Bosmajian Applied Chemistry Division Annapolis, Maryland 21401	1
Naval Ocean Systems Center Attn: Dr. S. Yamamoto Marine Sciences Division San Diego, California 91232	1
Dr. David L. Nelson Chemistry Program Office of Naval Research 800 North Quincy Street Arlington, Virginia 22217	1
Naval Ocean Systems Center Attn: Technical Library San Diego, California 92152	1
Naval Weapons Center Attn: Dr. A. B. Amster Chemistry Division China Lake, California 93555	1
Scientific Advisor Commandant of the Marine Corps Code RD-1 Washington, D.C. 20380	1
Dean William Tolles Naval Postgraduate School Monterey, California 93940	1
U.S. Army Research Office Attn: CRD-AA-IP P.O. Box 12211 Research Triangle Park, NC 27709	1
Mr. Vincent Schaper DTNSRDC Code 2830 Annapolis, Maryland 21402	1
Mr. John Boyle Materials Branch Naval Ship Engineering Center Philadelphia, Pennsylvania 19112	1
Mr. A. M. Anzalone Administrative Librarian PLASTEC/ARRADCOM Bldg 3401 Dover, New Jersey 07801	1

DL/413/83/01
056/413-2

TECHNICAL REPORT DISTRIBUTION LIST, 056

Dr. G. A. Somorjai
Department of Chemistry
University of California
Berkeley, California 94720

Dr. J. Murday
Naval Research Laboratory
Surface Chemistry Division (6170)
455 Overlook Avenue, S.W.
Washington, D.C. 20375

Dr. J. B. Hudson
Materials Division
Rensselaer Polytechnic Institute
Troy, New York 12181

Dr. Theodore E. Madey
Surface Chemistry Section
Department of Commerce
National Bureau of Standards
Washington, D.C. 20234

Dr. Chia-wei Woo
Department of Physics
Northwestern University
Evanston, Illinois 60201

Dr. Robert M. Hexter
Department of Chemistry
University of Minnesota
Minneapolis, Minnesota

Dr. J. E. Demuth
IBM Corporation
Thomas J. Watson Research Center
P.O. Box 218
Yorktown Heights, New York 10598

Dr. M. G. Lagally
Department of Metallurgical
and Mining Engineering
University of Wisconsin
Madison, Wisconsin 53706

Dr. Adolph B. Amster
Chemistry Division
Naval Weapons Center
China Lake, California 93555

Dr. W. Kohn
Department of Physics
University of California, San Diego
La Jolla, California 92037

Dr. R. L. Park
Director, Center of Materials
Research
University of Maryland
College Park, Maryland 20742

Dr. W. T. Peria
Electrical Engineering Department
University of Minnesota
Minneapolis, Minnesota 55455

Dr. Keith H. Johnson
Department of Metallurgy and
Materials Science
Massachusetts Institute of Technology
Cambridge, Massachusetts 02139

Dr. J. M. White
Department of Chemistry
University of Texas
Austin, Texas 78712

Dr. R. P. Van Duyne
Chemistry Department
Northwestern University
Evanston, Illinois 60201

Dr. S. Sibener
Department of Chemistry
James Franck Institute
5640 Ellis Avenue
Chicago, Illinois 60637

Dr. Arold Green
Quantum Surface Dynamics Branch
Code 3817
Naval Weapons Center
China Lake, California 93555

Dr. S. L. Bernasek
Princeton University
Department of Chemistry
Princeton, New Jersey 08544

DL/413/83/01
056/413-2

TECHNICAL REPORT DISTRIBUTION LIST, 056

Dr. F. Carter
Code 6132
Naval Research Laboratory
Washington, D.C. 20375

Dr. Richard Colton
Code 6112
Naval Research Laboratory
Washington, D.C. 20375

Dr. Dan Pierce
National Bureau of Standards
Optical Physics Division
Washington, D.C. 20234

Professor R. Stanley Williams
Department of Chemistry
University of California
Los Angeles, California 90024

Dr. R. P. Messmer
Materials Characterization Lab.
General Electric Company
Schenectady, New York ~~22217~~ 12301

Dr. Robert Gomer
Department of Chemistry
James Franck Institute
5640 Ellis Avenue
Chicago, Illinois 60637

Dr. Ronald Lee
R301
Naval Surface Weapons Center
White Oak
Silver Spring, Maryland 20910

Dr. Paul Schoen
Code 5570
Naval Research Laboratory
Washington, D.C. 20375

Dr. John T. Yates
Department of Chemistry
University of Pittsburgh
Pittsburgh, Pennsylvania 15260

Dr. Richard Greene
Code 5230
Naval Research Laboratory
Washington, D.C. 20375

Dr. L. Kesmodel
Department of Physics
Indiana University
Bloomington, Indiana 47403

Dr. K. C. Janda
California Institute of Technology
Division of Chemistry and Chemical Engineering
Pasadena, California 91125

Professor E. A. Irene
Department of Chemistry
University of North Carolina
Chapel Hill, Northc Carolina 27514

Dr. Adam Heller
Bell Laboratories
Murray Hill, New Jersey 07974

Dr. Martin Fleischmann
Department of Chemistry
Southampton University
Southampton S09 5NH
Hampshire, England

Dr. John W. Wilkins
Cornell University
Laboratory of Atomic and Solid State Physics
Ithaca, New York 14853

Dr. Richard Smardzewski
Code 6130
Naval Research Laboratory
Washington, D.C. 20375

DL/413/83/01
056/413-2

TECHNICAL REPORT DISTRIBUTION LIST, 056

Dr. R. G. Wallis
Department of Physics
University of California
Irvine, California 92664

Dr. D. Ramaker
Chemistry Department
George Washington University
Washington, D.C. 20052

Dr. P. Harsma
Physics Department
University of California
Santa Barbara, California 93106

Dr. J. C. Hemminger
Chemistry Department
University of California
Irvine, California 92717

Professor T. F. George
Chemistry Department
University of Rochester
Rochester, New York 14627

Dr. G. Rubloff
"BM"
Thomas J. Watson Research Center
P.O. Box 218
Yorktown Heights, New York 10598

Professor Horia Metiu
Chemistry Department
University of California
Santa Barbara, California 93106

Captain Lee Myers
AFOSR/NC
Bollig AFB
Washington, D.C. 20332

Professor Roald Hoffmann
Department of Chemistry
Cornell University
Ithaca, New York 14853

Dr. R. W. Plummer
Department of Physics
University of Pennsylvania
Philadelphia, Pennsylvania 19104

Dr. E. Yeager
Department of Chemistry
Case Western Reserve University
Cleveland, Ohio 41106

Professor D. Hercules
University Pittsburgh
Chemistry Department
Pittsburgh, Pennsylvania 15260

Professor N. Winograd
Department of Chemistry
Pennsylvania State University
University Park, Pennsylvania 16802

Dr. G. D. Stein
Mechanical Engineering Department
Northwestern University
Evanston, Illinois 60201

Professor A. Steckl
Department of Electrical and
Systems Engineering
Rensselaer Polytechnic Institute
Troy, NewYork 12181

Professor G. H. Morrison
Department of Chemistry
Cornell University
Ithaca, New York 14853

Dr. David Squire
Army Research Office
P.O. Box 12211
Research Triangle Park, NC 27709

END

FILMED

8-84

DTIC